THE JOURNAL OF PHYSICAL CHEMISTRY LETTERS
A JOURNAL OF THE AMERICAN CHEMICAL SOCIETY

pubs.acs.org/JPCL

Letter

Dissociation Mechanism of a Single O_2 Molecule Chemisorbed on Ag(110)

Minhui Lee, Emiko Kazuma,* Chi Zhang, Michael Trenary, Jun Takeya, Jaehoon Jung,* and Yousoo Kim*

Cite This: *J. Phys. Chem. Lett.* 2021, 12, 9868−9873

Read Online

ACCESS | Metrics & More | Article Recommendations | Supporting Information

ABSTRACT: The dissociation of O_2 molecules chemisorbed on silver surfaces is an essential reaction in industry, and the dissociation mechanism has long attracted attention. The detailed dissociation mechanism was studied at the single-molecule level on Ag(110) by using a scanning tunneling microscope (STM). The dissociation reaction was found to be predominantly triggered by inelastically tunneled holes from the STM tip due to the significantly distributed density of states below the Fermi level of the substrate. A combination of action spectroscopy with the STM and density functional theory calculations revealed that the O_2 dissociation reaction is caused by direct ladder-climbing excitation of the high-order overtones of the O−O stretching mode arising from anharmonicity enhanced by molecule−surface interactions.

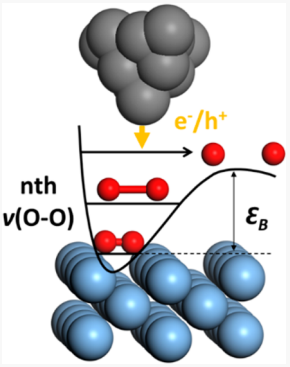

Obtaining mechanistic insights into molecular reactions on metal surfaces is important for understanding heterogeneous catalytic processes and for deepening our knowledge of fundamental surface elementary processes of the molecules.[1−3] The dissociation reaction of O_2 on Ag catalyst surfaces has long been of great interest in both fundamental research and industrial applications as a key process in heterogeneous oxidation catalysis.[1,4,5] In particular, Ag(110) has been intensively used for O_2 dissociation studies as it is the most reactive among the low-Miller-index Ag surfaces.[6] Early studies discovered three adsorbed states of O_2 on Ag(110) according to substrate temperature, which are physisorbed (<40 K), chemisorbed (40−150 K), and dissociatively chemisorbed (>150 K) states.[7] Molecular beam experiments revealed that the molecular adsorption of O_2 on Ag(110) is an activated process and that the chemisorbed state is a precursor to dissociation.[8,9] It is therefore important to clarify the dissociation mechanism and pathway of the chemisorbed O_2 molecules. However, the details of the reaction mechanism and excitation pathway responsible for the dissociation of O_2 chemisorbed on Ag(110) have not yet been identified.[9−20]

Conventional thermal processes leading to molecular reactions on surfaces are mainly explained in terms of vibrational ladder climbing, step-by-step sequential excitation, of a reaction coordinate (RC) mode of the adsorbed molecules. Single-molecule vibrational studies with a scanning tunneling microscope (STM) allow us to explore mechanistic details of surface chemical reactions.[21] Inelastic electron tunneling spectroscopy with STM (STM-IETS)[22] has been widely used to obtain the vibrational spectra of single molecules. In addition, action spectroscopy with STM (STM-AS)[23,24] provides an efficient means to investigate the vibrationally mediated excitation channels responsible for specific molecular motions or reactions induced by inelastically tunneled charge carriers from the STM tip. The underlying excitation pathways can be revealed by quantitative analysis of characteristic features of action spectra (Figures S1 and S2).[25] Various vibrational excitations can induce reactions as shown in Figure S1, and comprehensive interpretation with action spectra will provide the reaction mechanism.

Here we present a mechanistic study of the dissociation of O_2 on Ag(110) that reveals details of the reaction pathway. Comprehensive investigations using STM-IETS, STM-AS, and density functional theory (DFT) calculations show that the O−O bond dissociation of O_2 on Ag(110) occurs via direct ladder-climbing excitation of high overtone modes.

All experiments were performed by using a low-temperature STM (LT-STM, Omicron GmbH) with a W tip under ultrahigh vacuum (UHV) (<5×10^{-11} Torr) at ∼5 K. The single-crystal Ag(110) surface was cleaned by cycles of Ar^+ ion sputtering and annealing at 753 K. An atomically resolved STM image of the clean Ag(110) surface is shown in Figure S3a. The substrate was positioned on a cold stage maintained

Received: July 28, 2021
Accepted: September 30, 2021
Published: October 4, 2021

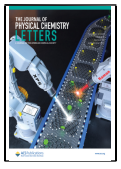

https://doi.org/10.1021/acs.jpclett.1c02456
J. Phys. Chem. Lett. 2021, 12, 9868−9873

at 89 K during O_2 dosing to induce molecular chemisorption on the Ag(110) surface,[7] followed by cooling to ~5 K.

STM images show that O_2 molecules chemisorb on the Ag(110) surface in two orientations, $O_2[001]$ and $O_2[1\bar{1}0]$ (Figure 1a,b and Figure S3b). STM images of $O_2[001]$ and $O_2[1\bar{1}0]$ acquired with a bare tip show oval and circular depressions along the Ag$[1\bar{1}0]$ axis, respectively, which coincide with those reported in previous experimental and theoretical studies.[14,15,26−28] The most stable adsorption site for both orientations is a hollow site,[29,30] as shown in Figure 1b.

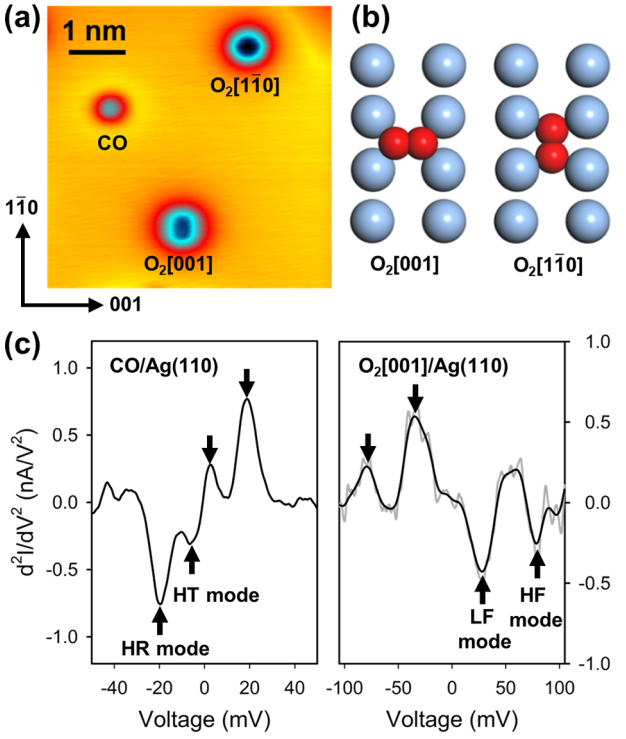

Figure 1. (a) Topographic STM image of CO and O_2 molecules on an Ag(110) surface (V = 20 mV, I_t = 0.1 nA). (b) Optimized adsorption structures of $O_2[001]$ and $O_2[1\bar{1}0]$ based on PBE-D3 calculations. (c) STM-IETS spectra for a CO molecule (left panel) and an $O_2[001]$ molecule (right panel) on Ag(110) after background subtraction. Spectra were obtained by averaging 11 scans from −50 to 50 mV and from −105 to 105 mV, respectively. Arrows in the left panel of (c) indicate the peak positions of hindered translation (HT) and hindered rotation (HR) modes. Arrows in the right panel of (c) indicate the peak positions of low-frequency (LF) and high-frequency (HF) modes. Gray and black curves are the raw data of the IETS spectra and the data after smoothing using a simple moving average method, respectively.

We performed STM-IETS experiments to obtain information about the vibrational properties of adsorbed O_2. To begin with, we acquired the spectrum of a coadsorbed CO molecule (Figure 1a) to verify the tip condition. This spectrum (Figure 1c, left panel) agrees well with one reported previously;[25] its peaks are assigned to the hindered translation (HT) and hindered rotation (HR) modes. We then acquired the STM-IETS spectrum of an $O_2[001]$ molecule in the same scan area (Figure 1a) with the same tip conditions. This spectrum exhibits negative and positive conductance changes at positive and negative sample biases, respectively (Figure 1c, right panel). The assignment of the dip at 78.8 mV and the peak at −78.8 mV (HF mode) to the ν(O−O) vibration agrees with previous studies reporting a vibrational mode at 82.0 meV based on STM-IETS data[30] and 85 meV based on electron energy loss spectroscopy.[12] The vibrational mode at the lower frequency corresponds to the antisymmetric Ag−O_2 stretching vibration, which has previously been studied by STM-IETS and theoretical calculations.[19,30] In contrast, the energies of the vibrational modes for $O_2[1\bar{1}0]$ could not be evaluated by STM-IETS due to a poor signal-to-noise (S/N) ratio, as also reported previously.[28,30]

To investigate the dissociation reaction of O_2 on Ag(110) at the single-molecule level, we injected electrons (holes) from the STM tip to a molecule at a positive (negative) sample bias voltage (V). Applying a voltage pulse at V = 360 mV to an $O_2[001]$ molecule induced dissociation of the O−O bond, resulting in the formation of two O atoms adsorbed at hollow sites (Figure 2a,b). Similarly, the dissociation of an $O_2[1\bar{1}0]$ molecule occurred at V = 460 mV (Figure 2b,c), and both dissociated O atoms adsorbed at hollow sites along the Ag$[1\bar{1}0]$ axis. The dissociated O atoms were located on the crystal axis to which the parent O_2 molecule originally adsorbed. These dissociation reactions of $O_2[001]$ and $O_2[1\bar{1}0]$ were also observed upon applying negative bias voltages (Figure S4).

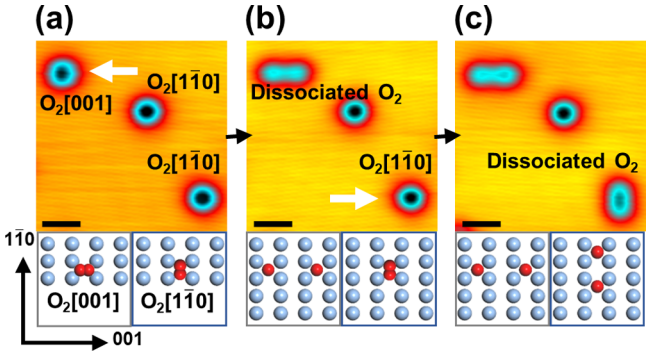

Figure 2. Topographic STM images (V = 20 mV, I_t = 0.1 nA) and structural models of the sample before (a) and after dissociation of the target (b) $O_2[001]$ and (c) $O_2[1\bar{1}0]$ molecules (marked with white arrows) induced by applying positive sample bias voltage pulses.

Figure 3a−d shows the STM action spectra for the dissociation of $O_2[001]$ and $O_2[1\bar{1}0]$ on Ag(110), i.e., the sample bias voltage dependence of the dissociation yield (Y), measured with both negative and positive biases. Y is defined as $Y = eR/I_t$, where R (= $1/t$) and I_t are the reaction rate and tunneling current, respectively. The time required for the reaction of a single molecule (t) is read from the corresponding current trace measurement (see Figure S5). Y differed significantly between negative and positive biases for both $O_2[001]$ and $O_2[1\bar{1}0]$. This can be explained in terms of the theory of STM-AS based on an adsorbate-induced resonance model[31] in which the electronic states of the adsorbate are temporarily occupied by tunneling electrons or holes, causing resonant excitation of the vibrational mode. According to the adsorbate-induced resonance model, the probability of vibrational excitation depends on the LDOS distribution of the adsorbate at the corresponding energy. Thus, we can interpret the bias polarity dependence of Y on the basis of the distribution of LDOS.[21,31] The distributions of the LDOS for $O_2[001]$ and $O_2[1\bar{1}0]$ obtained from our DFT

https://doi.org/10.1021/acs.jpclett.1c02456
J. Phys. Chem. Lett. 2021, 12, 9868−9873

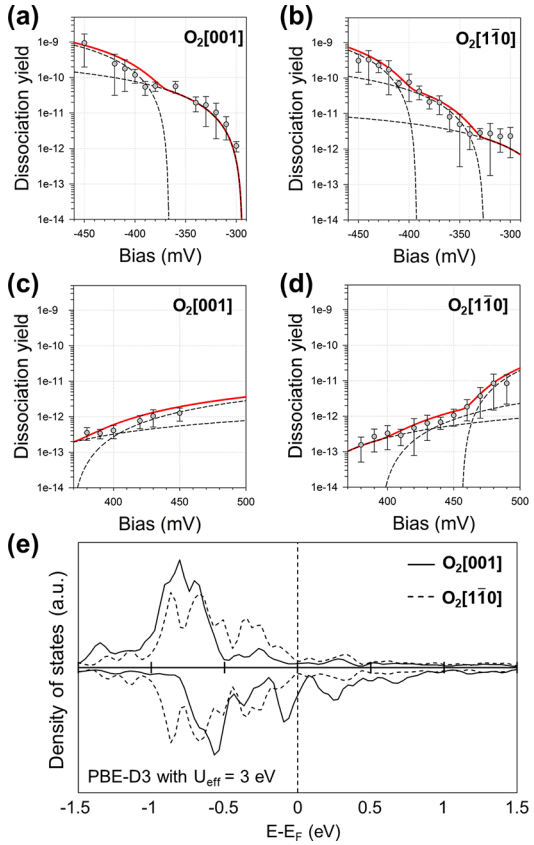

Figure 3. Action spectra for the dissociation of $O_2[001]$ in the negative (a) and positive (c) bias regions and for the dissociation of $O_2[1\bar{1}0]$ in the negative (b) and positive (d) bias regions. The initial tunneling current was set to 10 nA. Spectral fitting results are shown as red solid curves. (e) LDOS of an $O_2[001]$ (solid lines) and $O_2[1\bar{1}0]$ molecule (dotted lines) on the Ag(110) surface calculated by using PBE-D3. The on-site Coulomb potential was applied to the oxygen 2p states with the DFT+U scheme (U_{eff} = 3 eV).

calculations indicate that the LDOS of an O_2 molecule above E_F is much smaller than that below E_F (Figure 3e). The lower Y obtained in the positive bias region reflects the low LDOS of the O_2 molecule above E_F.

Spectral fitting of STM action spectra allowed us to derive fundamental information about the O_2 dissociation mechanism. Y can be defined as $Y(V) = K_{eff}\frac{f(V, \hbar\Omega, \sigma_{ph})^n}{V}$, where K_{eff}, $\hbar\Omega$, σ_{ph}, and n represent the effective prefactor, the vibrational energy responsible for the excitation, the vibrational broadening factor, and the reaction order, respectively. The $f(V, \hbar\Omega, \sigma_{ph})^n$ function (given in the Supporting Information) can be derived by twice integration of the effective vibrational DOS, assumed to be a Gaussian function of V.[32] To determine n, we examined the current dependence of $R(I)$, which exhibits a power-law dependence on I and n, $R(I) \propto I_t^n$,[33−35] as shown in Figure S6. The estimated values of n for $O_2[001]$ ($O_2[1\bar{1}0]$) are 2.24 (2.18) and 1.97 (2.01) at −320 and −430 mV, respectively. This implies that O_2 dissociation on Ag(110) requires two electrons at those bias voltages. In other words, two times the sequential excitation is necessary to overcome the reaction barrier. Table S1 shows the values of the fitting parameters K_{eff}, $\hbar\Omega$, σ_{ph}, and n that give the best fits to the STM action spectra. The fitting curves, indicated by solid and dashed lines in Figure 3a−d, show the estimated vibrational energies at −294 and ±367 meV for $O_2[001]$ and at −326, ±393, and +456 meV for $O_2[1\bar{1}0]$. These estimated resonant energies are much larger than the energies required for the fundamental transition (v = 1 ← 0) of O_2 on Ag(110)[12,30] based on the STM-IETS data (Figure 1c, right panel). The vibrational energies estimated by the spectral fitting of STM-AS data are thus suggested as ν(O−O) overtones of the RC mode, i.e., transitions to higher vibrationally excited states. These results indicate that the anharmonicity enhanced by the interaction between an adsorbate and a metal surface can play a crucial role in determining the excitation channels of a chemisorbed molecule on a metal surface.

To obtain further mechanistic insight into O_2 dissociation on Ag(110), we analyzed the STM-AS and STM-IETS results by considering anharmonicity on a potential energy surface. The anharmonicity increases significantly with the vibrational quantum number of the excited state but is also expected to be enhanced by the adsorbate−surface interaction. The vibrational energy levels for an anharmonic potential, such as the Morse potential, are written as $E_v = \hbar\omega_e\left(v + \frac{1}{2}\right) - \hbar\omega_e\chi_e\left(v + \frac{1}{2}\right)^2$, where v, $\hbar\omega_e$, and χ_e are the vibrational quantum number, harmonic vibrational energy, and anharmonicity constant, respectively. Table 1 presents the vibrational energies

Table 1. Vibrational Energies for $O_2[001]$ and $O_2[1\bar{1}0]$ Obtained Experimentally and by Spectral Fitting Estimation[a]

$O_2[001]$	experimental results (meV)	estimated values (meV)
v = 1	78.8 (IETS)	78.1
v = 5	−294.0 (AS)	311.5
v = 6	±367.0 (AS)	350.2
$O_2[1\bar{1}0]$	experimental results (meV)	estimated values (meV)
v = 1		77.2
v = 6	−326.0 (AS)	359.0
v = 7	±393.0 (AS)	394.5
v = 8	+456.0 (AS)	423.1

[a]The signs of the vibrational energies determined by STM-AS indicate the bias region of the corresponding STM action spectrum.

measured from STM-IETS and STM-AS, which were used for fitting to the equation above for E_v to obtain the anharmonicity and the corresponding estimated values (see the Supporting Information for the details of the fitting method). We used the vibrational energy of the first ν(O−O) mode of $O_2[001]$ as determined by STM-IETS for both adsorption orientations because the difference between the first vibrational energies of $O_2[001]$ and $O_2[1\bar{1}0]$ is expected to have a negligible impact on the fitting process given the much larger deviations expected for higher excited states due to anharmonicity.[17−19,36] The $\hbar\omega_e$ and χ_e terms were obtained by fitting the experimental data with the equation above for an anharmonic oscillator; the values for $O_2[001]$ ($O_2[1\bar{1}0]$) are $\hbar\omega_e$ = 85.99 ± 6.62 meV and $\chi_e = 4.59 \times 10^{-2} \pm 1.10 \times 10^{-2}$ with R^2 = 0.9134 ($\hbar\omega_e$ = 84.14 ± 6.52 meV and $\chi_e = 4.13 \times 10^{-2} \pm 0.81 \times 10^{-2}$ with R^2 = 0.8754). The estimated values for the first vibrationally excited state $E_{1\leftarrow0}$ for $O_2[001]$ and $O_2[1\bar{1}0]$ are 78.1 and 77.2 meV, respectively (Table 1). The $E_{1\leftarrow0}$ for $O_2[001]$ (78.1 meV) agrees well with the energy of the ν(O−O) mode (78.8 meV) determined by STM-IETS (Figure 1c,

https://doi.org/10.1021/acs.jpclett.1c02456
J. Phys. Chem. Lett. 2021, 12, 9868−9873

right panel). For $O_2[1\bar{1}0]$, the $E_{1\leftarrow0}$ is estimated to be 77.2 meV, although we could not evaluate the vibrational energies by STM-IETS due to the low S/N ratio. Additionally, the estimated χ_e values agree well with the value of 4×10^{-2} previously determined by electron energy loss spectroscopy[37] and are almost an order of magnitude greater than those of both gas-phase O_2 (7.6×10^{-3}) and O_2 physisorbed on Ag (8.3×10^{-3}),[38,39] as expected. The dissociation barrier (D_0) can also be obtained from χ_e of the Morse oscillator ($D_e = \frac{\hbar\omega_e}{4\chi_e}$, zero-point energy (ZPE) $= \frac{1}{2}\hbar\omega_e - \frac{1}{4}\hbar\omega_e\chi_e$, and $D_0 = D_e -$ ZPE) and is consistent with the reaction barrier (ε_B) for dissociation of O_2 on Ag(110). The evaluated D_e, ZPE, and D_0 for $O_2[001]$ ($O_2[1\bar{1}0]$) are 0.47 ± 0.15 eV, 42.0 ± 3.3 meV, and 0.43 ± 0.15 eV (0.51 ± 0.20 eV, 41.2 ± 3.2 meV, and 0.47 ± 0.20 eV), respectively. The ν(O−O) energy for $O_2[1\bar{1}0]$ evaluated by using PBE-D3 calculations is also smaller than that for $O_2[001]$, consistent with the interpretation of the experimental data (Table S2). Additionally, $O_2[1\bar{1}0]$ has a longer O−O bond and a higher O_2 adsorption energy (E_{ads}) than $O_2[001]$ due to a larger charge transfer from the metal surface. Consequently, the vibrational energies estimated from the STM-AS data for $O_2[001]$ can be attributed to the excitation channels corresponding to the fourth ($v = 5 \leftarrow 0$) and fifth ($6 \leftarrow 0$) overtones of the ν(O−O) mode, and those for $O_2[1\bar{1}0]$ can be attributed to its fifth ($6 \leftarrow 0$), sixth ($7 \leftarrow 0$), and seventh ($8 \leftarrow 0$) overtones, as summarized in Table 1. This indicates that the reaction pathway of dissociation is direct overtone-mode excitation, which is shown in Figure S1c.

Figure 4 schematically depicts the vibrational excitation channels for the dissociation of $O_2[001]$ and $O_2[1\bar{1}0]$ molecules chemisorbed on Ag(110). Our STM-AS experiments successfully revealed two feasible excitation pathways for $O_2[001]$ and three for $O_2[1\bar{1}0]$ (Figure 3). Two-step excitations along all the observed overtone-mediated channels are required to provide enough energy to overcome the ε_B for dissociation of both $O_2[001]$ and $O_2[1\bar{1}0]$ on Ag(110), which was confirmed by the value of n (around 2) estimated from the current dependence of the rate (Figure S6). Although the vibrational relaxation rate is expected to be faster than the electron arrival rate, the population of molecules vibrationally excited by the first electron should still be high enough when the second electron arrives to yield the measured dissociation rate. However, because of the short vibrational lifetimes, dissociation by an $n = 1$ process would be expected to be faster than by an $n = 2$ process. Therefore, based on the channels illustrated in Figure 4, the ε_B values for O_2 dissociation were estimated to be $430 < \varepsilon_B < 588$ meV for $O_2[001]$ and $456 < \varepsilon_B < 640$ meV for $O_2[1\bar{1}0]$, which agree well with the D_0 values obtained by fitting the experimental data with the equation of the Morse oscillator. It is noteworthy that our study experimentally reports the ε_B values separately for both $O_2[001]$ and $O_2[1\bar{1}0]$ for the first time to the best of our knowledge, which are comparable with the reported values in previous experimental and theoretical studies (Table S3). Our experimental results clearly show not only that the high-order ν(O−O) overtone modes can serve as excitation channels for the dissociation of O_2 on Ag(110) but also that tunneling holes ($V < 0$) are >100 times more efficient than tunneling electrons as an excitation source (Figure 3). The dependence of reaction efficiency on the choice of excitation source can be explained by the distribution of electronic states around E_F, as mentioned above.[31]

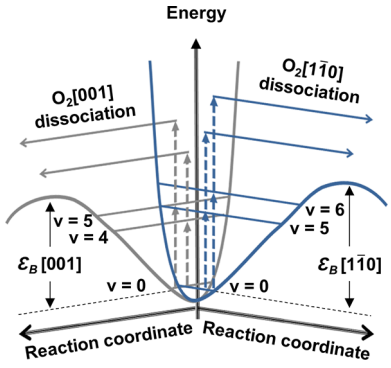

Figure 4. Schematic representation of the dissociation channels for $O_2[001]$ and $O_2[1\bar{1}0]$ molecules chemisorbed on Ag(110). Dissociation occurs via direct excitation of high-order O−O stretching overtone modes. The dissociation channel for $O_2[1\bar{1}0]$ via the sixth ($8 \leftarrow 0$) overtone is omitted for clarity.

In conclusion, we have shown that the dissociation mechanism of O_2 molecules chemisorbed on Ag(110) corresponds to direct excitations of the high-order ν(O−O) overtone modes. In addition, the dissociation barriers were experimentally estimated based on the Morse oscillator potential energy with anharmonicity at the single-molecule level. It is meaningful that we construct the potential energy surface for dissociation by state-selective experiments at a single-molecule level. Considering the short lifetime of vibrationally excited states and the enhanced anharmonicity of molecules chemisorbed on metal surfaces, it is reasonable that overtone excitation rather than sequential single excitations is needed to overcome the relatively high reaction barrier. The LDOS distribution below E_F explains why the reaction efficiency depended on the choice of excitation carrier as observed in the STM-AS experiment. Our study shows the roles of overtones and efficient excitation carriers for surface reaction dynamics, which should be considered when developing models of the reaction mechanism.

■ ASSOCIATED CONTENT

Supporting Information

The Supporting Information is available free of charge at https://pubs.acs.org/doi/10.1021/acs.jpclett.1c02456.

Proposed excitation pathways of chemical reactions and molecular motions on metal surfaces, formula of spectral fitting, anharmonic potential fitting using the Morse oscillator, computation details, Figures S1−S8, and Tables S1−S3 (PDF)

■ AUTHOR INFORMATION

Corresponding Authors

Emiko Kazuma − *Surface and Interface Science Laboratory, RIKEN, Wako, Saitama 351-0198, Japan;* orcid.org/0000-0003-0834-9832; Email: emiko.kazuma@riken.jp

Jaehoon Jung − *Department of Chemistry, University of Ulsan, Ulsan 44776, Republic of Korea;* orcid.org/0000-0001-6550-139X; Email: jjung2015@ulsan.ac.kr

Yousoo Kim − *Surface and Interface Science Laboratory, RIKEN, Wako, Saitama 351-0198, Japan;* orcid.org/0000-0001-7730-0704; Email: ykim@riken.jp

https://doi.org/10.1021/acs.jpclett.1c02456
J. Phys. Chem. Lett. 2021, 12, 9868−9873

Authors

Minhui Lee − *Surface and Interface Science Laboratory, RIKEN, Wako, Saitama 351-0198, Japan; Department of Advanced Materials Science, School of Frontier Sciences, The University of Tokyo, Kashiwa, Chiba 277-8561, Japan;* orcid.org/0000-0001-7217-5334

Chi Zhang − *Surface and Interface Science Laboratory, RIKEN, Wako, Saitama 351-0198, Japan*

Michael Trenary − *Department of Chemistry, University of Illinois at Chicago, Chicago, Illinois 60607, United States;* orcid.org/0000-0003-1419-9252

Jun Takeya − *Department of Advanced Materials Science, School of Frontier Sciences, The University of Tokyo, Kashiwa, Chiba 277-8561, Japan*

Complete contact information is available at: https://pubs.acs.org/10.1021/acs.jpclett.1c02456

Notes

The authors declare no competing financial interest.

■ ACKNOWLEDGMENTS

We are grateful for the use of the HOKUSAI-GreatWave supercomputer system of RIKEN. The authors appreciate Y. Hasegawa and Y. Shimizu for supporting the preparation of W tips. The present work was supported by the RIKEN Junior Research Associate Program and in part by KAKENHI (18H01947 and 18H05257). J.J. acknowledges the financial support of National Research Foundation of Korea (NRF-2021R1A2C1009191). M.T. acknowledges support from a grant from the US National Science Foundation (CHE-2102622).

■ REFERENCES

(1) Lefferts, L.; van Ommen, J. G.; Ross, J. R. H. The Oxidative Dehydrogenation of Methanol to Formaldehyde over Silver Catalysts in Relation to the Oxygen-Silver Interaction. *Appl. Catal.* **1986**, *23* (2), 385−402.

(2) Roberts, M. W. Chemisorption and Reaction Pathways at Metal Surfaces: The Role of Surface Oxygen. *Chem. Soc. Rev.* **1989**, *18* (0), 451−475.

(3) Hendriksen, B. L. M.; Bobaru, S. C.; Frenken, J. W. M. Oscillatory Co Oxidation on Pd(100) Studied with in Situ Scanning Tunneling Microscopy. *Surf. Sci.* **2004**, *552* (1), 229−242.

(4) Campbell, C. T.; Paffett, M. T. Model Studies of Ethylene Epoxidation Catalyzed by the Ag(110) Surface. *Surf. Sci.* **1984**, *139* (2−3), 396−416.

(5) Serafin, J. G.; Liu, A. C.; Seyedmonir, S. R. Surface Science and the Silver-Catalyzed Epoxidation of Ethylene: An Industrial Perspective. *J. Mol. Catal. A: Chem.* **1998**, *131* (1−3), 157−168.

(6) Montemore, M. M.; van Spronsen, M. A.; Madix, R. J.; Friend, C. M. O_2 Activation by Metal Surfaces: Implications for Bonding and Reactivity on Heterogeneous Catalysts. *Chem. Rev.* **2018**, *118* (5), 2816−2862.

(7) Prince, K. C.; Paolucci, G.; Bradshaw, A. M. Oxygen Adsorption on Silver (110): Dispersion, Bonding and Precursor State. *Surf. Sci.* **1986**, *175* (1), 101−122.

(8) Vattuone, L.; Rocca, M.; Boragno, C.; Valbusa, U. Initial Sticking Coefficient of O_2 on Ag(110). *J. Chem. Phys.* **1994**, *101* (1), 713−725.

(9) Lončarić, I.; Alducin, M.; Juaristi, J. I. Dissociative Dynamics of O_2 on Ag(110). *Phys. Chem. Chem. Phys.* **2015**, *17* (14), 9436−45.

(10) Campbell, C. T. Atomic and Molecular Oxygen Adsorption on Ag(111). *Surf. Sci.* **1985**, *157* (1), 43−60.

(11) Åkerlund, C.; Zorić, I.; Kasemo, B.; Cupolillo, A.; de Mongeot, F. B.; Rocca, M. Dissociation of O_2 Chemisorbed on Ag (110) and Pt(111) Induced by Energetic Xe Atoms. *Chem. Phys. Lett.* **1997**, *270* (1−2), 157−162.

(12) Bartolucci, F.; Franchy, R.; Barnard, J. C.; Palmer, R. E. Two Chemisorbed Species of O_2 on Ag(110). *Phys. Rev. Lett.* **1998**, *80* (23), 5224−5227.

(13) Hahn, J. R.; Ho, W. Chemisorption and Dissociation of Single Oxygen Molecules on Ag(110). *J. Chem. Phys.* **2005**, *123* (21), 214702.

(14) Hahn, J. R.; Ho, W. Orbital Specific Chemistry: Controlling the Pathway in Single-Molecule Dissociation. *J. Chem. Phys.* **2005**, *122* (24), 244704.

(15) Hahn, J. R.; Jang, S. H.; Kim, K. W.; Son, S. B. Hot Carrier-Selective Chemical Reactions on Ag(110). *J. Chem. Phys.* **2013**, *139* (7), 074707.

(16) Gravil, P. A.; Bird, D. M.; White, J. A. Adsorption and Dissociation of O_2 on Ag(110). *Phys. Rev. Lett.* **1996**, *77* (18), 3933−3936.

(17) Bird, D. M.; Gravil, P. A. First-Principles Calculations of Molecular Dissociation at Surfaces. *Surf. Sci.* **1997**, *377* (1−3), 555−562.

(18) Roy, S.; Mujica, V.; Ratner, M. A. Chemistry at Molecular Junctions: Rotation and Dissociation of O_2 on the Ag(110) Surface Induced by a Scanning Tunneling Microscope. *J. Chem. Phys.* **2013**, *139* (7), 074702.

(19) Rawal, T. B.; Hong, S.; Pulkkinen, A.; Alatalo, M.; Rahman, T. S. Adsorption, Diffusion, and Vibration of Oxygen on Ag(110). *Phys. Rev. B: Condens. Matter Mater. Phys.* **2015**, *92* (3), 035444.

(20) Lončarić, I.; Alducin, M.; Juaristi, J. I. Molecular Dynamics Simulation of O_2 Adsorption on Ag(110) from First Principles Electronic Structure Calculations. *Phys. Chem. Chem. Phys.* **2016**, *18* (39), 27366−27376.

(21) Kim, Y.; Motobayashi, K.; Frederiksen, T.; Ueba, H.; Kawai, M. Action Spectroscopy for Single-Molecule Reactions − Experiments and Theory. *Prog. Surf. Sci.* **2015**, *90* (2), 85−143.

(22) Stipe, B. C.; Rezaei, M. A.; Ho, W. Single-Molecule Vibrational Spectroscopy and Microscopy. *Science* **1998**, *280* (5370), 1732−5.

(23) Kawai, M.; Komeda, T.; Kim, Y.; Sainoo, Y.; Katano, S. Single-Molecule Reactions and Spectroscopy Via Vibrational Excitation. *Philos. Trans. R. Soc., A* **2004**, *362* (1819), 1163−1171.

(24) Choi, Y. S.; Kim, T.-S.; Petek, H.; Yoshihara, K.; Christensen, R. L. Evidence for Quantization of the Transition State for *cis*−*trans* Isomerization. *J. Chem. Phys.* **1994**, *100* (12), 9269−9271.

(25) Oh, J.; Lim, H.; Arafune, R.; Jung, J.; Kawai, M.; Kim, Y. Lateral Hopping of Co on Ag(110) by Multiple Overtone Excitation. *Phys. Rev. Lett.* **2016**, *116* (5), 056101.

(26) Olsson, F. E.; Lorente, N.; Persson, M. Stm Images of Molecularly and Atomically Chemisorbed Oxygen on Silver. *Surf. Sci.* **2003**, *522* (1−3), L27−L35.

(27) Alducin, M.; Sánchez-Portal, D.; Arnau, A.; Lorente, N. Mixed-Valency Signature in Vibrational Inelastic Electron Tunneling Spectroscopy. *Phys. Rev. Lett.* **2010**, *104* (13), 136101.

(28) Monturet, S.; Alducin, M.; Lorente, N. Role of Molecular Electronic Structure in Inelastic Electron Tunneling Spectroscopy: O_2 on Ag(110). *Phys. Rev. B: Condens. Matter Mater. Phys.* **2010**, *82* (8), 085447.

(29) Barth, J. V.; Zambelli, T.; Wintterlin, J.; Schuster, R.; Ertl, G. Direct Observation of Mobility and Interactions of Oxygen Molecules Chemisorbed on the Ag(110) Surface. *Phys. Rev. B: Condens. Matter Mater. Phys.* **1997**, *55* (19), 12902−12905.

(30) Hahn, J. R.; Lee, H. J.; Ho, W. Electronic Resonance and Symmetry in Single-Molecule Inelastic Electron Tunneling. *Phys. Rev. Lett.* **2000**, *85* (9), 1914−1917.

(31) Frederiksen, T.; Paulsson, M.; Ueba, H. Theory of Action Spectroscopy for Single-Molecule Reactions Induced by Vibrational Excitations with Stm. *Phys. Rev. B: Condens. Matter Mater. Phys.* **2014**, *89* (3), 035427.

(32) Motobayashi, K.; Kim, Y.; Ueba, H.; Kawai, M. Insight into Action Spectroscopy for Single Molecule Motion and Reactions

through Inelastic Electron Tunneling. *Phys. Rev. Lett.* **2010**, *105* (7), 076101.
(33) Stipe, B. C.; Rezaei, M. A.; Ho, W.; Gao, S.; Persson, M.; Lundqvist, B. I. Single-Molecule Dissociation by Tunneling Electrons. *Phys. Rev. Lett.* **1997**, *78* (23), 4410−4413.
(34) Stipe, B. C.; Rezaei, M. A.; Ho, W. Inducing and Viewing the Rotational Motion of a Single Molecule. *Science* **1998**, *279* (5358), 1907−9.
(35) Kim, Y.; Komeda, T.; Kawai, M. Single-Molecule Reaction and Characterization by Vibrational Excitation. *Phys. Rev. Lett.* **2002**, *89* (12), 126104.
(36) Loncaric, I.; Alducin, M.; Juaristi, J. I. Molecular Dynamics Simulation of O_2 Adsorption on Ag(110) from First Principles Electronic Structure Calculations. *Phys. Chem. Chem. Phys.* **2016**, *18* (39), 27366−27376.
(37) Vattuone, L.; Rocca, M.; Valbusa, U. Anharmonic Shift in the Stretching Frequency of O_2 Chemisorbed on Ag (110). *Surf. Sci.* **1994**, *314* (3), L904−L908.
(38) Schmeisser, D.; Demuth, J. E.; Avouris, Ph. Electron-Energy-Loss Studies of Physisorbed O_2 and N_2 on Ag and Cu Surfaces. *Phys. Rev. B: Condens. Matter Mater. Phys.* **1982**, *26* (9), 4857−4863.
(39) Buatier de Mongeot, F.; Cupolillo, A.; Valbusa, U.; Rocca, M. Anharmonicity of the O_2−Ag(001) Chemisorption Potential. *J. Chem. Phys.* **1997**, *106* (22), 9297−9304.

https://doi.org/10.1021/acs.jpclett.1c02456
J. Phys. Chem. Lett. 2021, 12, 9868−9873